

Appendix to:  
Evaluating An Estimated New Keynesian Small Open Economy  
Model

Malin Adolfson  
Sveriges Riksbank

Stefan Laséen  
Sveriges Riksbank

Jesper Lindé\*  
Sveriges Riksbank and CEPR

Mattias Villani  
Sveriges Riksbank and Stockholm University

---

\* *Corresponding author:* Sveriges Riksbank, SE-103 37 Stockholm, Sweden. Tel.: + 46 8 787 08 73; fax: +46 8 21 05 31. Email address: [jesper.linde@riksbank.se](mailto:jesper.linde@riksbank.se)

## Appendix A. Estimation results

### A.1. Prior vs. posterior plots

Figures A.1a to A.1c report the prior and posterior distributions for all estimated parameters in the model including the modified UIP condition and using a flexible Taylor-type instrument rule to model the pre-inflation targeting regime (i.e., the last model in Table 1). In accordance with the results in Table 1, the figures show that the data is generally informative about the parameters, as the posterior distributions differ from the priors, with a few exceptions (i.e.,  $\xi_w$  and  $r_\pi$ ). The results for these parameters are discussed in greater detail in the main text.

### A.2. Raw Metropolis chains

In Figures A.2a to A.2c we report the 500,000 post burn-in Metropolis draws for each parameter. The Markov chain in Figure A.2 show that there are no clear trends or correlations between the parameters in the model.

The CUSUM plots of the Metropolis draws are depicted in Figures A.3a to A.3c. The solid line (labeled posterior) is the accumulated mean of the draws, while the dashed line (labeled average) is a window average of the last 50,000 draws. As expected from the raw Metropolis draws, the CUSUM plots show no sign of a trending mean in the parameters throughout the whole chain. Even if the window averages are varying slightly, there do not appear to be any high correlation between the different parameters. In particular, we notice from Figures A.2 and A.3 that the risk premium parameters  $\tilde{\phi}_s$ ,  $\rho_{\tilde{\phi}}$  and  $\sigma_{\tilde{\phi}}$  do not show any clear sign of cross-correlation or time-varying means, supporting the discussion in the main text that these parameters are well identified.

### A.3. Sequential log marginal likelihoods

In Figure A.4, we plot the log marginal likelihood sequentially for each 50,000th draw, using all the preceding iterations in the computation of the marginal likelihood with the modified harmonic estimator in Geweke (1999).<sup>1</sup> The lines pertain to eight different probabilities of the truncated ellipsoids of the joint posterior distribution. As can be seen from Figure A.4, the spread between the largest and smallest ellipsoids is not very large after a couple of 100,000 draws. It is also clear from the figure that the marginal likelihood converges after about 200,000 draws. To obtain convergence, we found it to be of critical importance to obtain a good estimate of the Hessian matrix. We start by maximizing the posterior density and evaluating the Hessian matrix at the posterior mode using standard numerical optimization routines. Prior to the optimization we transform all the parameters to the unconstrained domain (we use logit transformations on parameters restricted to the unit interval, and a log transformation for strictly positive parameters). Second, draws from the posterior distribution are generated using the Metropolis-Hastings algorithm.

---

<sup>1</sup>The marginal likelihood of a model  $i$  is defined as  $m_i = \int L_i(\theta_i; x) p_i(\theta_i) d\theta_i$ , where  $L_i(\theta_i; x)$  is the usual likelihood function of the model's parameter vector conditional on the observed data  $x$ .  $p_i(\theta_i)$  is the prior distribution of the model's parameters.  $m_i$  is the unconditional probability of the observed data, under the assumed prior distribution, and is therefore a measure of model fit. The marginal likelihood is a relative measure and should be compared across competing models. The Bayes factor comparing two models  $i$  and  $j$  is defined as  $B_{ij} = m_i/m_j$ .

#### A.4. Multivariate ANOVA

In Figure A.5, we report the multivariate potential scale reduction factor (MPSRF) based on four independent Metropolis chains with different starting values consisting of 500,000 draws each. The analysis is based on subsampling every 5th draw for computational reasons. Gelman et al. (1995) argue that by rule-of-thumb, the MPSRF should be less than 1.1 to have a satisfactory convergence. As is evident from Figure A.5, this requirement is fulfilled in our chains after about 100,000 draws (i.e, after 20,000 iterations in the plot), and after about 250,000 draws it is down to less than 1.05. Figure A.5 also depicts the total variance in all the four Markov chains together with the variance within each parallel chain. As the number of draws increases we see that the difference between the total and within variation in the parallel chains decreases.

#### A.5. Contour plots

In the main text, we argue from using uniform priors and comparing Bayesian model probabilities that the parameters associated with the UIP condition,  $\tilde{\phi}_s$  and  $\rho_{\tilde{\phi}}$ , are well identified given our set of observable variables in the measurement equation. In Figure A.6 we show contour plots of the likelihood function in the  $\{\tilde{\phi}_s, \rho_{\tilde{\phi}}\}$ -space conditional on the posterior median of the other parameters. Figure A.6a shows the likelihood for different values of  $\tilde{\phi}_s$  and  $\rho_{\tilde{\phi}}$  using the entire set of 15 observables. The data is relatively informative about the intrinsic persistence  $\tilde{\phi}_s$  but has less to say about the exogenous autocorrelation  $\rho_{\tilde{\phi}}$ . Even if the likelihood in Figure A.6a is nearly constant in the neighborhood of the posterior mode, the likelihood function appear to be well shaped when all the other parameters are not kept fixed. When plotting the likelihood contours using *only* the real exchange rate in the measurement equation, we see that the data is even less informative about  $\rho_{\tilde{\phi}}$  (see Figure A.6b).  $\rho_{\tilde{\phi}}$  can take on almost any value for small values of  $\tilde{\phi}_s$ , and the likelihood function in this case suggest a corner solution of  $(\tilde{\phi}_s = 1, \rho_{\tilde{\phi}} = 0)$ .

#### A.6. Measurement errors

In order to examine the sensitivity of our results to the choice of including measurement errors in the estimation, we provide in Table A.1 the posterior mode estimates when varying the size of the measurement errors. For ease of comparison we also include the baseline case. As a first sensitivity check we set the variance of the measurement errors to 0.05 percent for all the domestic variables and 0 for the foreign variables (i.e., less than half of what we are using in the baseline case in the main text). From the table we see that this does not change the parameter estimates by much. However, when treating the data as being measured almost perfectly (setting the variance of the measurement errors to 0.01 percent for the domestic variables, see the last column) certain parameters shift, sometimes substantially from an economic viewpoint. For example, the price stickiness parameter increases from 0.82 to 0.92 and the substitution elasticity between investment goods drops from 2.67 to 1.28. However, given that we know there are measurement problems in the Swedish data we are using, it is not surprising that the estimates change somewhat when no measurement errors are included in the estimation. Statistics Sweden has made several alterations in how they collect their price statistics and we were for example not able to remove all the seasonal variation in the GDP deflator. We therefore believe that a small amount of measurement errors is reasonable to include in the estimation. It should also be noted that it is the fundamental shocks in the model that explain the major part of the variability in the data. In Figure A.7 we plot the actual data against the fluctuations generated by the model without any measurement errors. As can be seen from the figure the two series

are very similar, so the measurement errors account only for a small fraction of the variability in the data.

### A.7. Unconditional moments

To get a better sense for the modified UIP condition's compliance to the data we provide in Table A.2 a posterior predictive analysis for the real exchange rate. The table shows the unconditional moments for the real exchange rate in the data and in the two DSGE models (the latter computed from simulated data in the model with the standard UIP condition and in the model with the modified UIP condition, respectively). The table indicates that the specification with the modified UIP condition captures the autocorrelation of the real exchange rate in the actual data but overpredicts the volatility somewhat, while the specification with a standard UIP underpredicts both the persistence and the volatility in the real exchange rate. However, it should be noted that we are probably considering a too short sample period for making the second moments a sufficiently informative statistic to truly evaluate the empirical coherence of the models. This is particular the case if the transition from the fixed exchange rate regime to the inflation targeting regime should be taken into account.

## Appendix B. Misspecification analysis

### B.1. Using a VAR with a DSGE prior

To describe the DSGE-VAR approach in some detail, let the VAR model with  $p$  lags be denoted

$$y_t = \Phi_0 + \Phi_w w_t + \Phi_1 y_{t-1} + \dots + \Phi_p y_{t-p} + u_t = \Phi' x_t + u_t, \quad t = 1, \dots, T, \quad (\text{B.1})$$

where  $y_t$  contains the  $n$  stationary endogenous variables (I(1) variables enter in first differences),  $w_t$  is a  $q$ -dimensional vector of exogenous variables,  $x'_t = (1, w'_t, y'_{t-1}, \dots, y'_{t-p})$ ,  $\Phi' = (\Phi_0, \Phi_w, \Phi_1, \dots, \Phi_p)$  and  $u_t \sim N(0, \Sigma_u)$  are independent across time. Del Negro and Schorfheide (2004) propose a prior for  $\Phi$  and  $\Sigma_u$  that one may think of as centered around OLS estimates based on a simulated data set of  $T^*$  observations from a DSGE model with parameter vector  $\theta$ . The posterior of the VAR coefficients may similarly be thought of as the result of applying a Bayesian VAR to the combined data set of actual and artificial data. Del Negro and Schorfheide (2004) avoid the simulation variability in the above mental sketch by replacing the simulated cross moment matrices  $\sum y_t y'_t$ ,  $\sum x_t x'_t$  and  $\sum x_t y'_t$  (which are the building blocks in the OLS estimates) with their population counterparts  $T^* E_\theta(y_t y'_t)$ ,  $T^* E_\theta(x_t x'_t)$  and  $T^* E_\theta(x_t y'_t)$ , respectively.  $E_\theta$  here denotes the expectation with respect to the DSGE model with parameter vector  $\theta$ . Formally, Del Negro and Schorfheide (2004) propose the following Normal-Inverted Wishart prior for  $\Phi$  and  $\Sigma_u$ , conditional on  $\theta$ ,

$$\begin{aligned} \Sigma_u | \theta &\sim IW[\lambda T \Sigma_u^*(\theta), \lambda T - k] \\ \text{vec } \Phi | \Sigma_u, \theta &\sim N \{ \text{vec } \Phi^*(\theta), \Sigma_u \otimes [\lambda T E_\theta(x_t x'_t)]^{-1} \} \end{aligned}$$

where the prior means of  $\Phi$  and  $\Sigma_u$  are computed from the DSGE moments:

$$\begin{aligned} \Phi^*(\theta) &= E_\theta^{-1}(x_t x'_t) E_\theta(x_t y'_t) \\ \Sigma_u^*(\theta) &= E_\theta(y'_t y_t) - E_\theta(y'_t x'_t) E_\theta^{-1}(x_t x'_t) E_\theta(x_t y'_t), \end{aligned}$$

$k = np + q + 1$  and  $\lambda = T^*/T$  is the ratio of the number of artificial DSGE observations to the number of observations in the actual data. This prior is proper if  $\lambda \geq \lambda_{\min} = (k + n)/T$ .<sup>2</sup>

As  $\lambda$  decreases, the posterior estimates of the VAR coefficients approach the unrestricted OLS estimates. It is important to understand that this does not mean that the corresponding limiting marginal likelihood can be interpreted as some kind of measure of fit for an unrestricted VAR. A marginal likelihood is always associated with a prior, which when  $\lambda = \lambda_{\min}$  is the prior which uses just enough DSGE observations to make it proper. As the marginal likelihood is the prior expectation of the likelihood function, it is clear that such a vague prior may be only weakly connected to more traditional measures of fit based on OLS estimates.

The regime shift in the DSGE model's monetary policy rule requires special attention in the DSGE-VAR analysis. Given that the DSGE model allows all the reduced form parameters to change as result of the regime shift, even if only a subset of the structural parameters change (i.e., the conduct of monetary policy), the same must be true in the VAR model. We therefore consider the following  $n$ -dimensional VAR with a potential break in all parameters at a known time point  $t = T_1$

$$y_t = \begin{cases} \Phi'_1 x_t + \varepsilon_t, & Cov(\varepsilon_t) = \Sigma_1 \quad \text{for } t \leq T_1 \\ \Phi'_2 x_t + \varepsilon_t, & Cov(\varepsilon_t) = \Sigma_2 \quad \text{for } t > T_1 \end{cases} \quad (\text{B.2})$$

A completely unrestricted estimation this model ignores that  $(\Phi_1, \Sigma_1)$  and  $(\Phi_2, \Sigma_2)$  coincide in all dimensions except those related to the monetary policy rule, and is therefore a nearly impossible task, given the limited data available in the two subperiods. An elegant solution is to use a Del Negro-Schorfheide type of prior centered on the DSGE model with a regime change in the monetary policy rule. If we assume that the two sets of parameters  $(\Phi_1, \Sigma_1)$  and  $(\Phi_2, \Sigma_2)$  are a priori independent conditional on the parameters of the DSGE model, then the results in Del Negro and Schorfheide (2004) are easily generalized to the extended model in (B.2). Although it is straightforward to use different prior tightness in the two subperiods, we restrict  $\lambda$  to be the same for all  $t$ . Note also that  $\lambda_{\min} = (k + n)/\min(T_1, T_2)$ , which may be rather large when at least one of  $T_1$  or  $T_2$  are small.

## B.2. VAR approximation error

The first step in the analysis is to determine how well a VAR/VECM with finite lag length can approximate the DSGE model. To investigate this we compare the autocovariance function of the DSGE-VAR and DSGE-VECM with  $\lambda = \infty$  (i.e. where  $\Phi = \Phi^*(\theta)$  and  $\Sigma_u = \Sigma_u^*(\theta)$ ) to the autocovariance function of the DSGE model with the modified UIP.<sup>3</sup> We use the posterior mode of the DSGE model as an estimate of  $\theta$ . The results for a VAR/VECM with four lags are displayed in Figure 8.<sup>4</sup> The general impression from Figure A.8 is that the VAR(4) is rather successful in approximating the autocovariances of the individual variables (diagonal subgraphs), but is not able to capture several of the cross-covariances between the variables. Note that

---

<sup>2</sup>This is a conjugate prior, so that the posterior of  $\Phi$  and  $\Sigma_u$  also belongs to the Normal-Inverted Wishart family, again conditional on  $\theta$ . This makes it possible to obtain a closed form expression for the marginal posterior of  $\theta$  (see Del Negro and Schorfheide, 2004). Posterior sampling from the marginal posterior of  $\theta$  may then be performed in exactly the same way as in the pure DSGE model. The main difference being that the time-consuming Kalman filtering of the state variables in the DSGE model are replaced by the less demanding computation of the DSGE cross-moments (see Del Negro and Schorfheide, 2004 for details on how these moments are computed by solving Lyapunov equations).

<sup>3</sup>The autocovariance function for the VECMs were computed from the MA representation of I(1) processes (the so called Granger representation) using the explicit expressions in Hansen (2005). The MA coefficients were truncated after 500 lags.

<sup>4</sup>In order to make the subplots visible we report results for a subset of variables included in the estimation but it is important to note that all variables are included in the VARs when computing the vector autocovariances.

the VAR by construction gives identical autocovariances as the DSGE model up to lag  $p$ , the lag length in the VAR. Experiments with a longer lag length in the VAR/VECM showed an increasing accuracy in the approximation, but we continue to use  $p = 4$  in the ensuing analysis as a longer lag length is unsuitable for estimation given the relatively short data set. Turning to the VECM(4) approximation in Figure A.8, it seems that the addition of cointegrating relations to the VAR helps to improve the approximation to the DSGE model.

### B.3. Assessing the role of the UIP condition

In order to examine the quantitative role of the modified UIP condition when the cross equation restrictions have been optimally relaxed, we compare in Figure A.9 the cross correlation functions in the DSGE-VECM model with the standard (solid) and modified UIP (dashed) condition for the optimal lambda ( $\hat{\lambda} = 7$ ). The figure also reports the standard deviation of the variables in the model with the standard UIP condition (in the bottom of the subgraphs) and in the model with the modified UIP condition (to the right of the subgraphs). From the figure we see that there are some differences remaining between the two specifications also in the hybrid model. In particular there are still differences between the cross correlations pertaining to the real exchange rate, although the induced volatility in the real exchange rate is a lot more similar between the two specifications of the VECM relative to the recorded difference between the structural DSGE models (cf. Figure A.9 and Table A.2 in this Appendix). However, the marginal likelihood comparison in Table 2 in the main paper suggest that the discrepancies in Figure A.9 are not jointly very important.

## References

- Del Negro, Marco, Frank Schorfheide (2004), “Priors from General Equilibrium Models for VARs”, *International Economic Review* 45(2), 643-673.
- Gelman, A., J. Carlin, H. Stern and D. Rubin (1995), *Bayesian Data Analysis*, Chapman & Hall, New York.
- Geweke, J. (1999), “Using Simulation Methods for Bayesian Econometrics Models: Inference, Development and Communication”, *Econometric Reviews* 18(1), 1-73.
- Hansen, P. (2005), “Granger’s representation theorem: A closed-form expression for I(1) processes”, *Econometrics Journal* 8, 23-38.

Table A.1: Posterior mode estimates under different sizes of measurement errors

Parameter		Baseline*		Variance (domestic measurement errors) = 0.05		Variance (domestic measurement errors) = 0.01	
		posterior mode	std dev. (Hessian)	posterior mode	std dev. (Hessian)	posterior mode	std dev. (Hessian)
Calvo wages	$\xi_w$	0.773	0.264	0.736	0.265	0.677	0.194
Calvo domestic prices	$\xi_d$	0.815	0.322	0.870	0.298	0.921	0.214
Calvo import cons. prices	$\xi_{m,c}$	0.899	0.182	0.902	0.173	0.899	0.163
Calvo import inv. prices	$\xi_{m,i}$	0.943	0.174	0.941	0.169	0.939	0.160
Calvo export prices	$\xi_x$	0.880	0.185	0.889	0.190	0.912	0.212
Indexation wages	$\kappa_w$	0.320	0.489	0.289	0.465	0.362	0.471
Indexation prices	$\kappa$	0.230	0.334	0.261	0.313	0.303	0.303
Markup domestic	$\lambda_d$	1.199	0.239	1.214	0.222	1.243	0.195
Markup imported cons.	$\lambda_{m,c}$	1.580	0.057	1.611	0.041	1.291	0.068
Markup imported invest.	$\lambda_{m,i}$	1.150	0.276	1.165	0.238	1.213	0.153
Investment adj. cost	$\tilde{S}^*$	8.811	1.326	8.761	1.334	7.808	1.354
Habit formation	$b$	0.638	0.264	0.644	0.254	0.686	0.265
Subst. elasticity invest.	$\eta_i$	2.672	0.168	2.389	0.136	1.280	0.143
Subst. elasticity foreign	$\eta_f$	1.491	0.271	1.492	0.273	1.547	0.310
Technology growth	$\mu_z$	1.005	0.047	1.005	0.047	1.005	0.048
Risk premium	$\tilde{\phi}$	0.042	0.478	0.042	0.468	0.057	0.445
UIP modification	$\tilde{\phi}_s$	0.607	0.236	0.612	0.238	0.621	0.292
Unit root tech. shock persistence	$\rho_{\mu_z}$	0.857	0.504	0.866	0.398	0.741	0.087
Stationary tech. shock persistence	$\rho_\varepsilon$	0.901	0.556	0.877	0.385	0.781	0.202
Invest. spec. tech shock persistence	$\rho_Y$	0.749	0.502	0.847	0.505	0.822	0.358
Asymmetric tech. shock persistence	$\rho_{z^*}$	0.962	0.257	0.938	0.288	0.775	0.081
Consumption pref. shock persistence	$\rho_{\xi_c}$	0.688	0.672	0.800	0.787	0.731	0.729
Labour supply shock persistence	$\rho_{\xi_h}$	0.266	0.340	0.259	0.338	0.518	0.197
Risk premium shock persistence	$\rho_{\tilde{\phi}}$	0.656	0.444	0.624	0.424	0.641	0.507
Unit root tech. shock standard deviation	$\sigma_{\mu_z}$	0.133	0.201	0.128	0.200	0.188	0.197
Stationary tech. shock standard deviation	$\sigma_\varepsilon$	0.681	0.124	0.838	0.091	1.065	0.086
Invest. spec. tech. shock standard deviation	$\sigma_Y$	0.360	0.195	0.318	0.162	0.375	0.143
Asymmetric tech. shock standard deviation	$\sigma_{z^*}$	0.188	0.144	0.188	0.144	0.204	0.160
Consumption pref. shock standard deviation	$\sigma_{\xi_c}$	0.243	0.184	0.250	0.169	0.236	0.157
Labour supply shock standard deviation	$\sigma_{\xi_h}$	0.380	0.102	0.385	0.098	0.348	0.107
Risk premium shock standard deviation	$\sigma_{\tilde{\phi}}$	0.790	0.254	0.904	0.245	0.965	0.276
Domestic markup shock standard deviation	$\sigma_{\lambda}$	0.800	0.104	0.799	0.099	0.853	0.108
Imp. cons. markup shock standard deviation	$\sigma_{\lambda_{m,c}}$	1.110	0.103	1.181	0.100	1.010	0.098
Imp. invest. markup shock standard deviation	$\sigma_{\lambda_{m,i}}$	1.147	0.109	1.127	0.105	0.959	0.095
Export markup shock standard deviation	$\sigma_{\lambda_x}$	1.037	0.133	1.060	0.130	1.042	0.143
Interest rate smoothing, pre-infl. targeting	$\rho_{R,1}$	0.883	0.231	0.882	0.229	0.889	0.238
Inflation response, pre-infl. targeting	$r_{\pi,1}$	1.694	0.142	1.683	0.145	1.697	0.141
Diff. infl response, pre-infl. targeting	$r_{\Delta\pi,1}$	0.159	0.054	0.145	0.052	0.116	0.051
Real exch. rate response, pre-infl. targeting	$r_{x,1}$	0.012	0.024	0.010	0.024	0.038	0.030
Output response, pre-infl. targeting	$r_{y,1}$	0.134	0.046	0.145	0.044	0.138	0.044
Diff. output response, pre-infl. targeting	$r_{\Delta y,1}$	0.111	0.044	0.103	0.040	0.052	0.022
Monetary policy shock, pre-infl. targeting	$\sigma_{R,1}$	0.386	0.150	0.369	0.154	0.386	0.149
Inflation target shock, pre-infl. targeting	$\sigma_{\pi^c,1}$	0.267	0.299	0.302	0.275	0.350	0.265
Interest rate smoothing	$\rho_{R,2}$	0.865	0.185	0.855	0.173	0.844	0.155
Inflation response	$r_{\pi,2}$	1.738	0.129	1.732	0.130	1.718	0.130
Diff. infl response	$r_{\Delta\pi,2}$	0.128	0.027	0.129	0.029	0.126	0.024
Real exch. rate response	$r_{x,2}$	-0.026	0.016	-0.026	0.014	-0.037	0.013
Output response	$r_{y,2}$	0.096	0.039	0.092	0.040	0.088	0.043
Diff. output response	$r_{\Delta y,2}$	0.101	0.030	0.083	0.031	0.096	0.027
Monetary policy shock	$\sigma_{R,2}$	0.101	0.117	0.101	0.130	0.089	0.117
Inflation target shock	$\sigma_{\pi^c,2}$	0.080	0.505	0.073	0.505	0.070	0.453

\*Note: The variance of the measurement errors in the baseline estimation is set to 0 for the foreign variables and the domestic interest rate, 0.1 percent for the real wage, consumption and output, and 0.2 percent for all the other variables.

Table A.2: Second moments for the real exchange rate, data and model

	Data (86Q1-04Q4)	Model standard UIP	Model modified UIP
Standard deviation	9.28	5.92 (3.79-9.52)	14.54 (7.34-27.79)
Autocorrelation	0.97	0.85 (0.67-0.94)	0.97 (0.93-0.99)

Note: For the model the median and 95 percent uncertainty intervals (in parenthesis) are reported from simulating the two model specifications 10.000 times with 76 periods each using different draws from the posterior distribution every time.



Figure A.1a: Prior and posterior distributions, friction parameters.

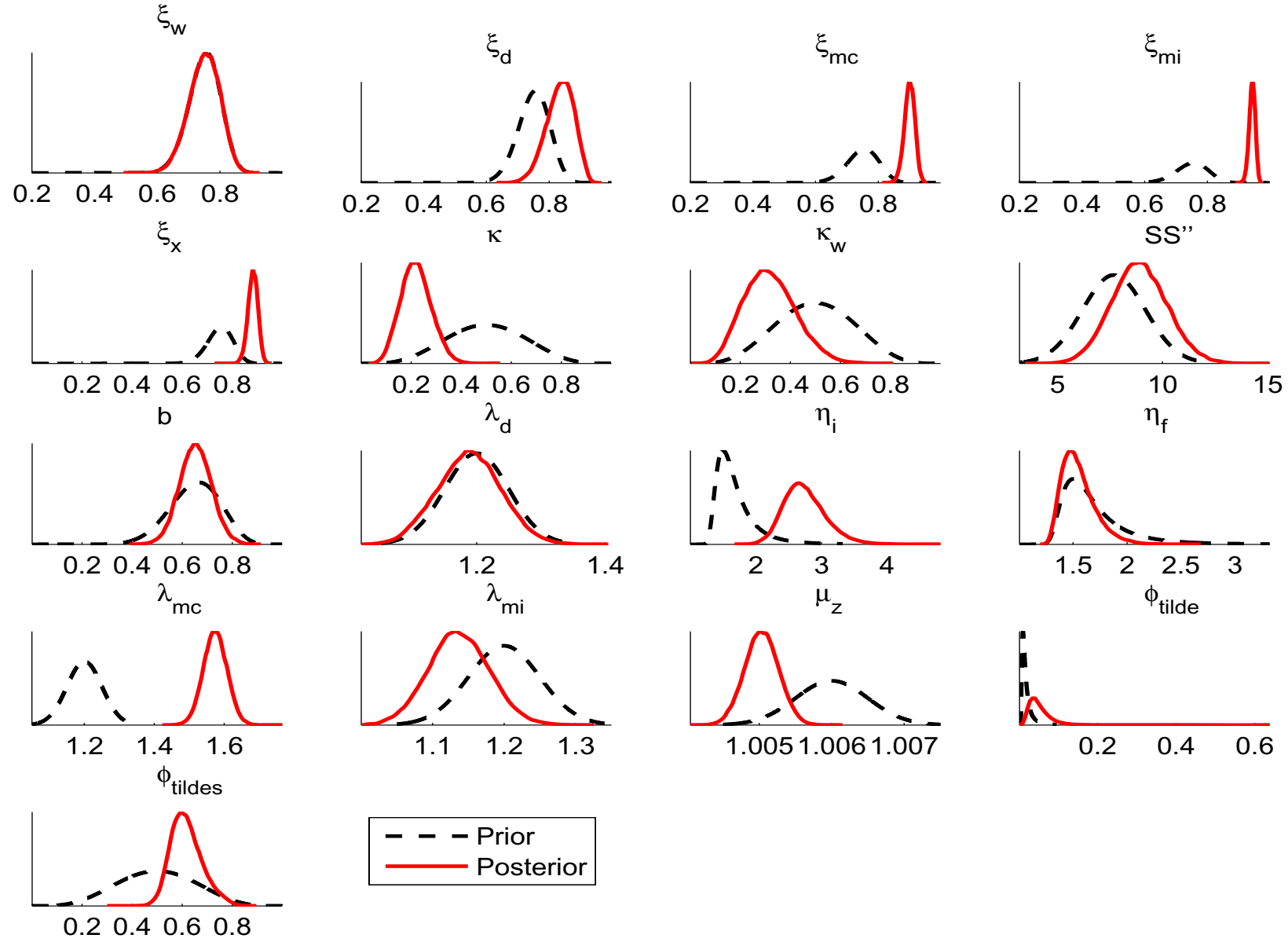


Figure A.1b: Prior and posterior distributions, shock parameters.

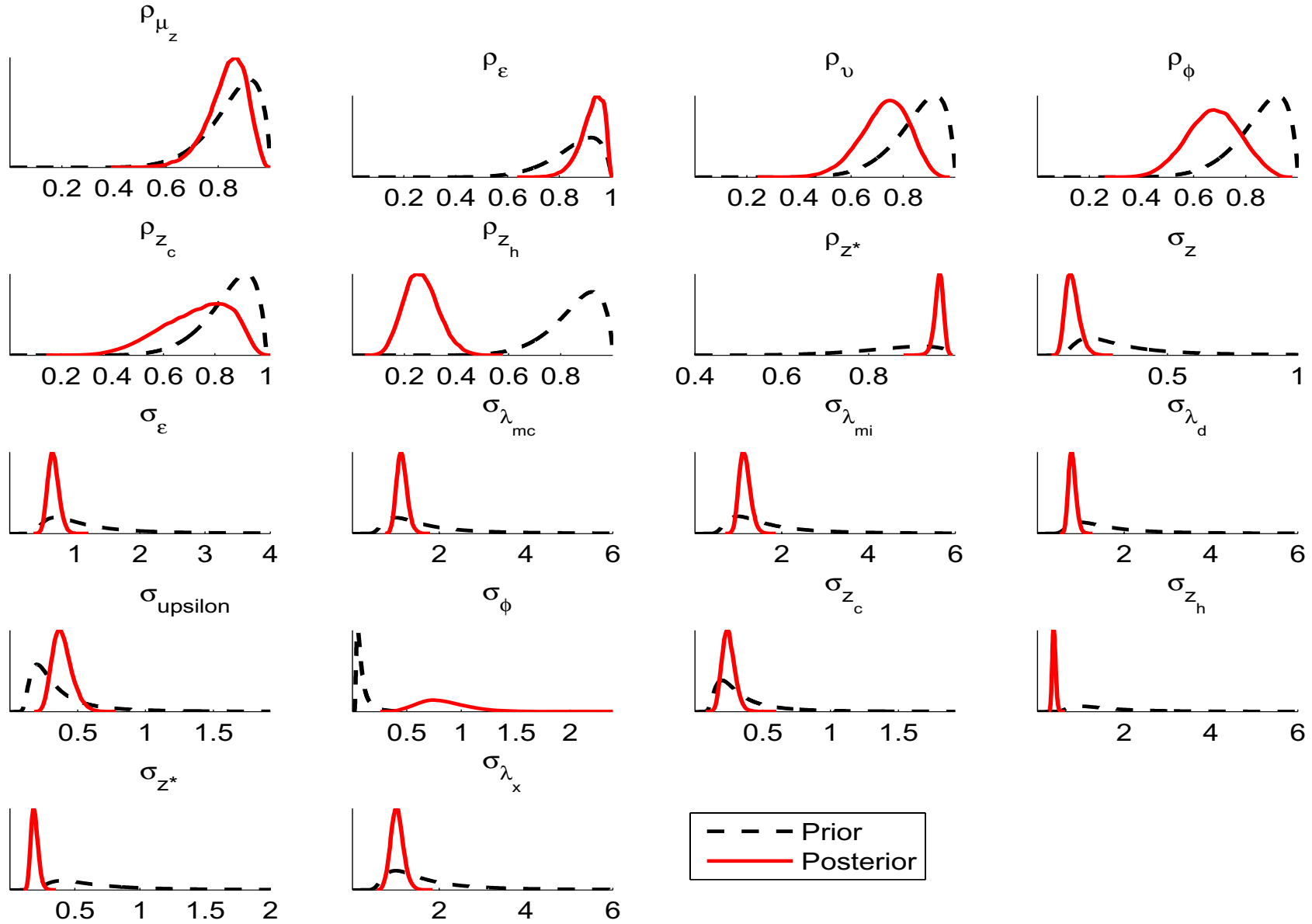


Figure A.1c: Prior and posterior distributions, policy parameters.

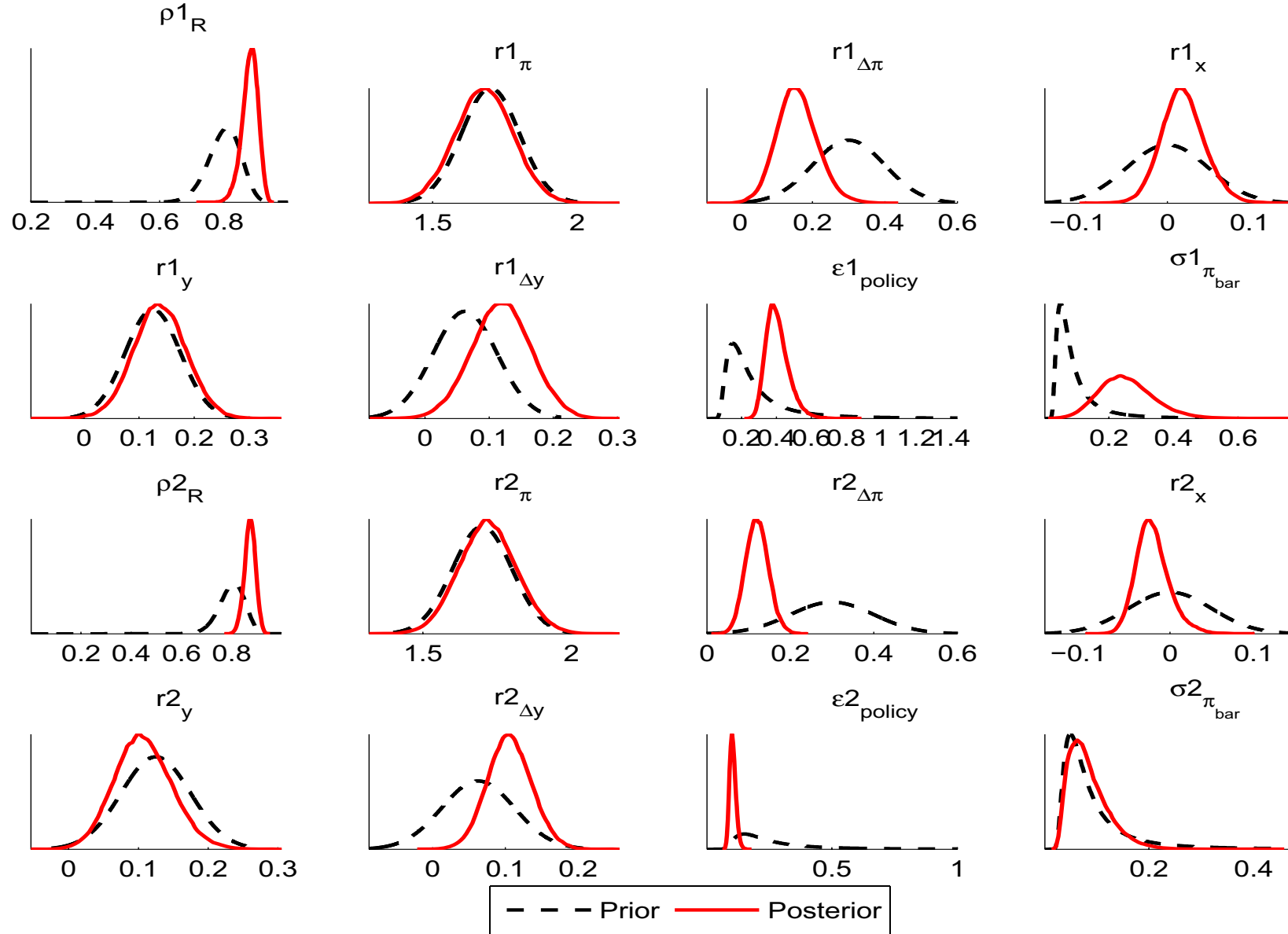


Figure A.2a: Plots of the raw Metropolis draws, friction parameters.

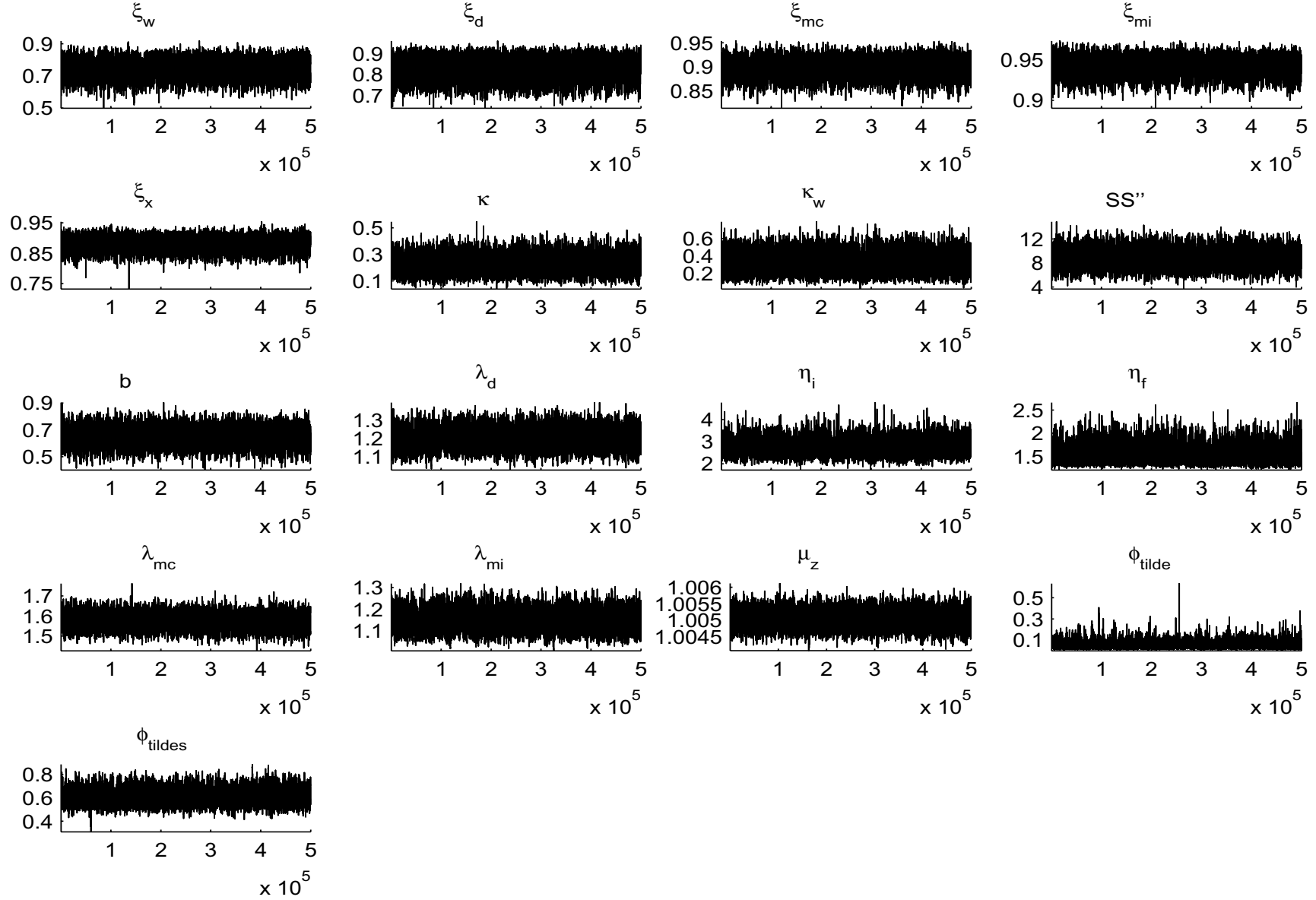


Figure A.2b: Plots of the raw Metropolis draws, shock parameters.

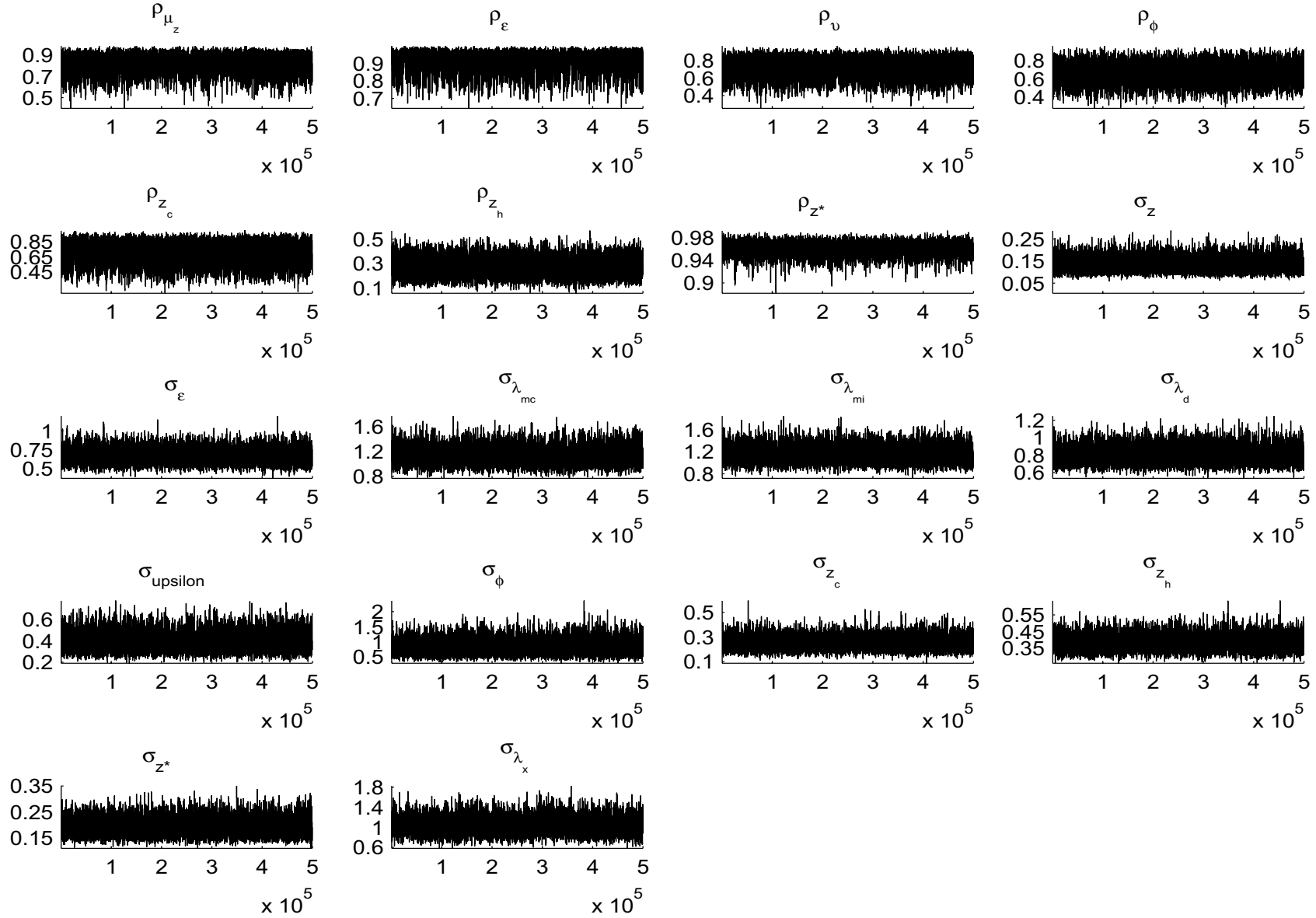


Figure A.2c: Plots of the raw Metropolis draws, policy parameters.

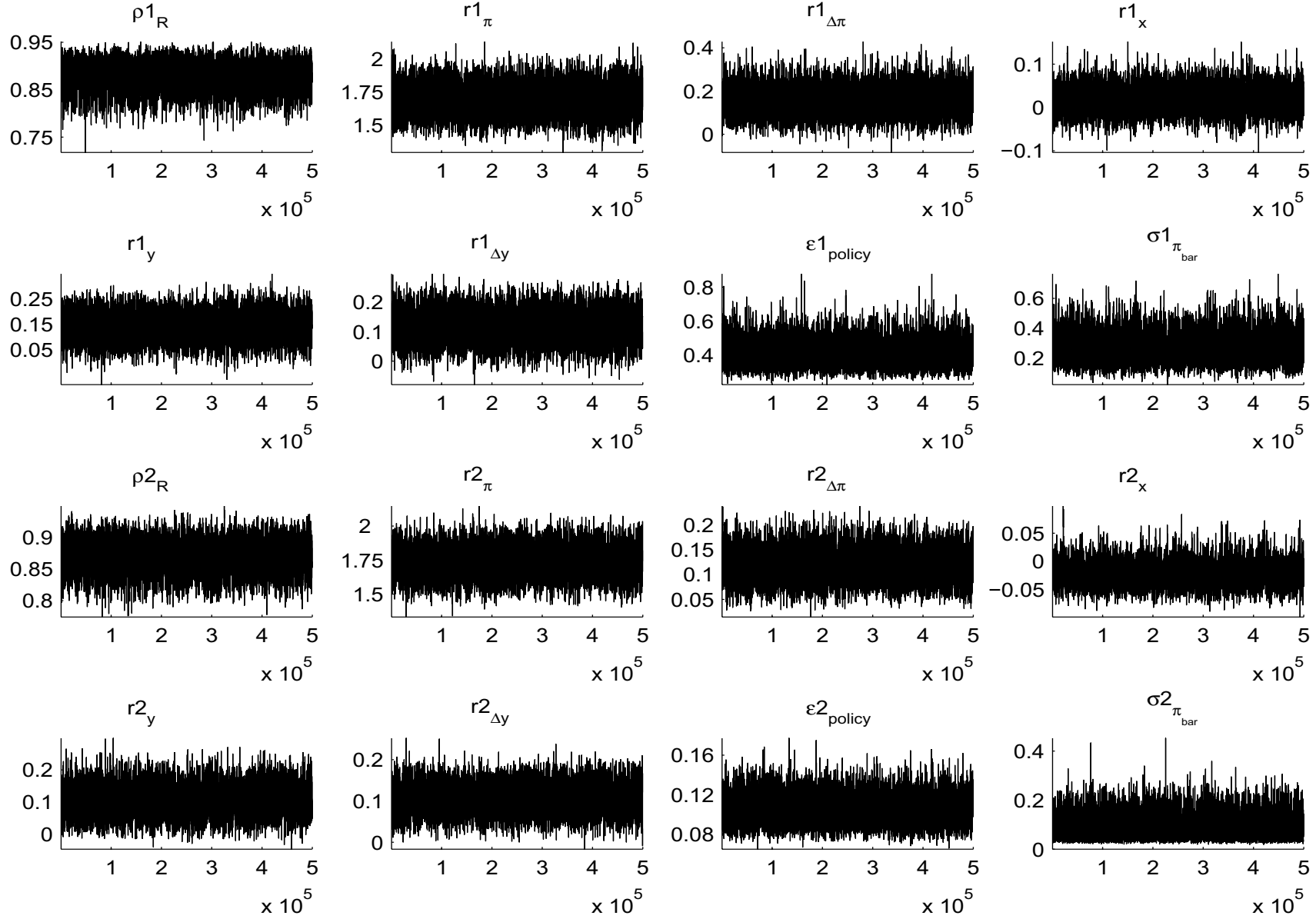


Figure A.3a: CUSUM plots of the Metropolis draws, friction parameters.

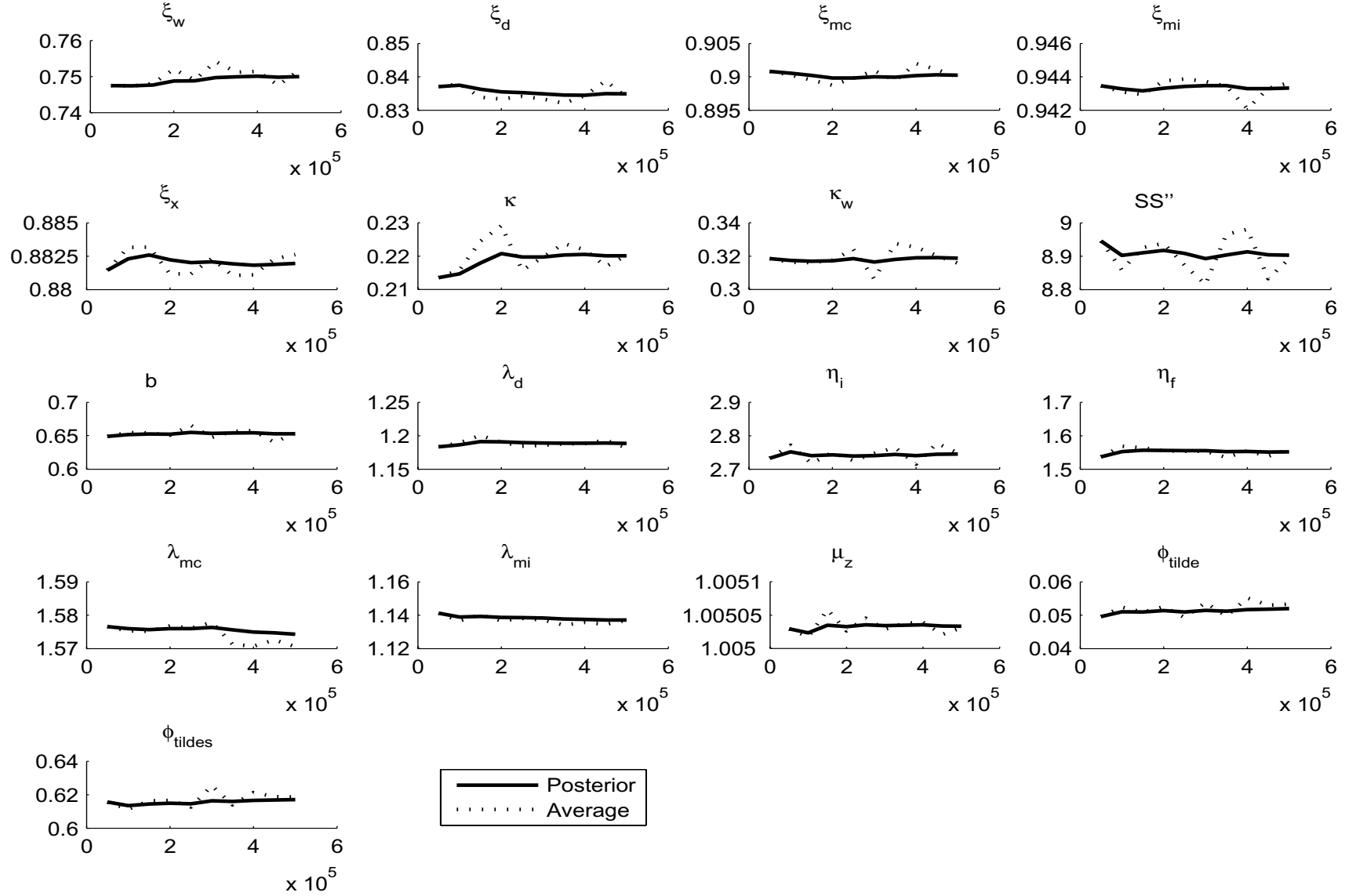


Figure A.3b: CUSUM plots of the Metropolis draws, shock parameters.

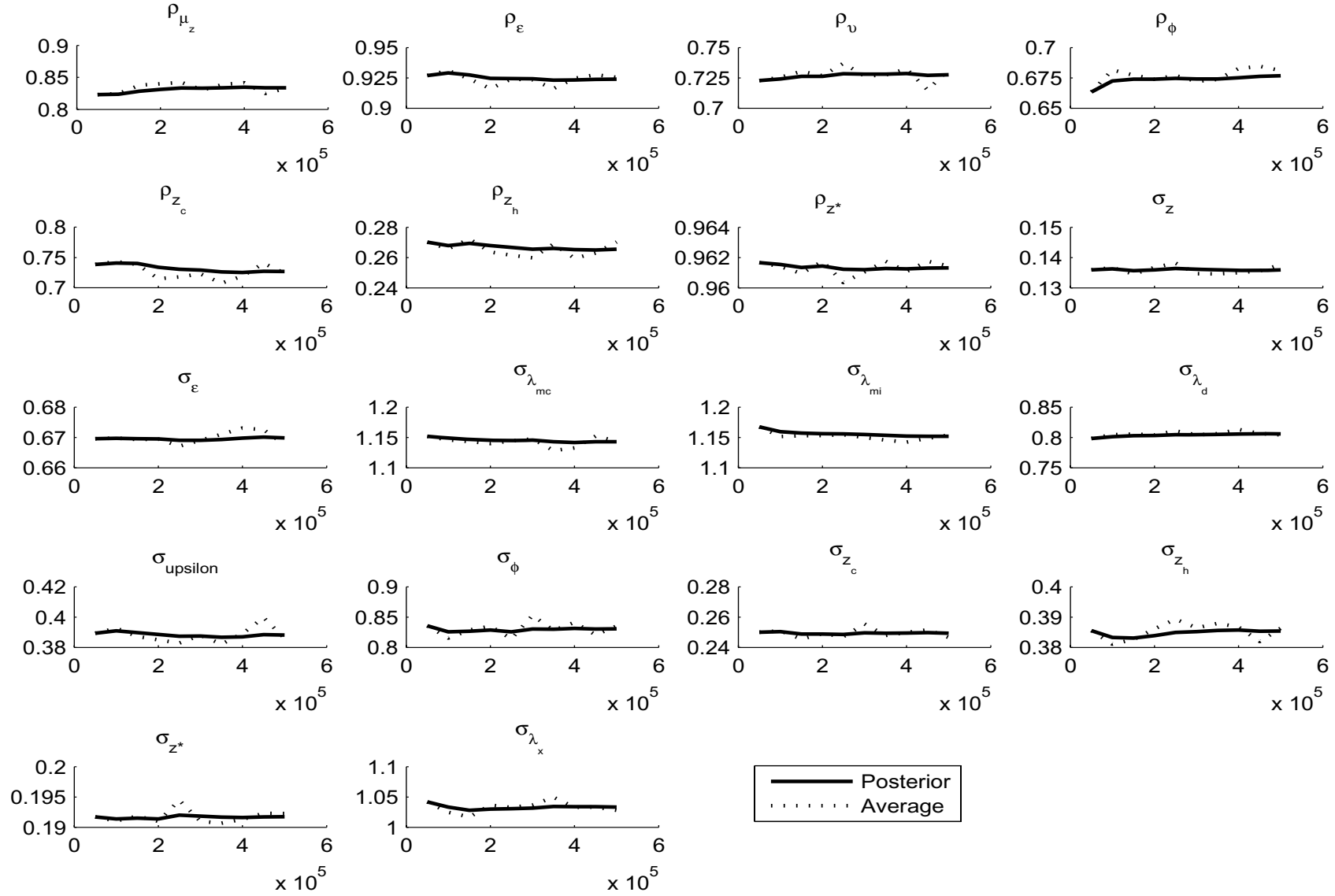




Figure A.3c: CUSUM plots of the Metropolis draws, policy parameters.

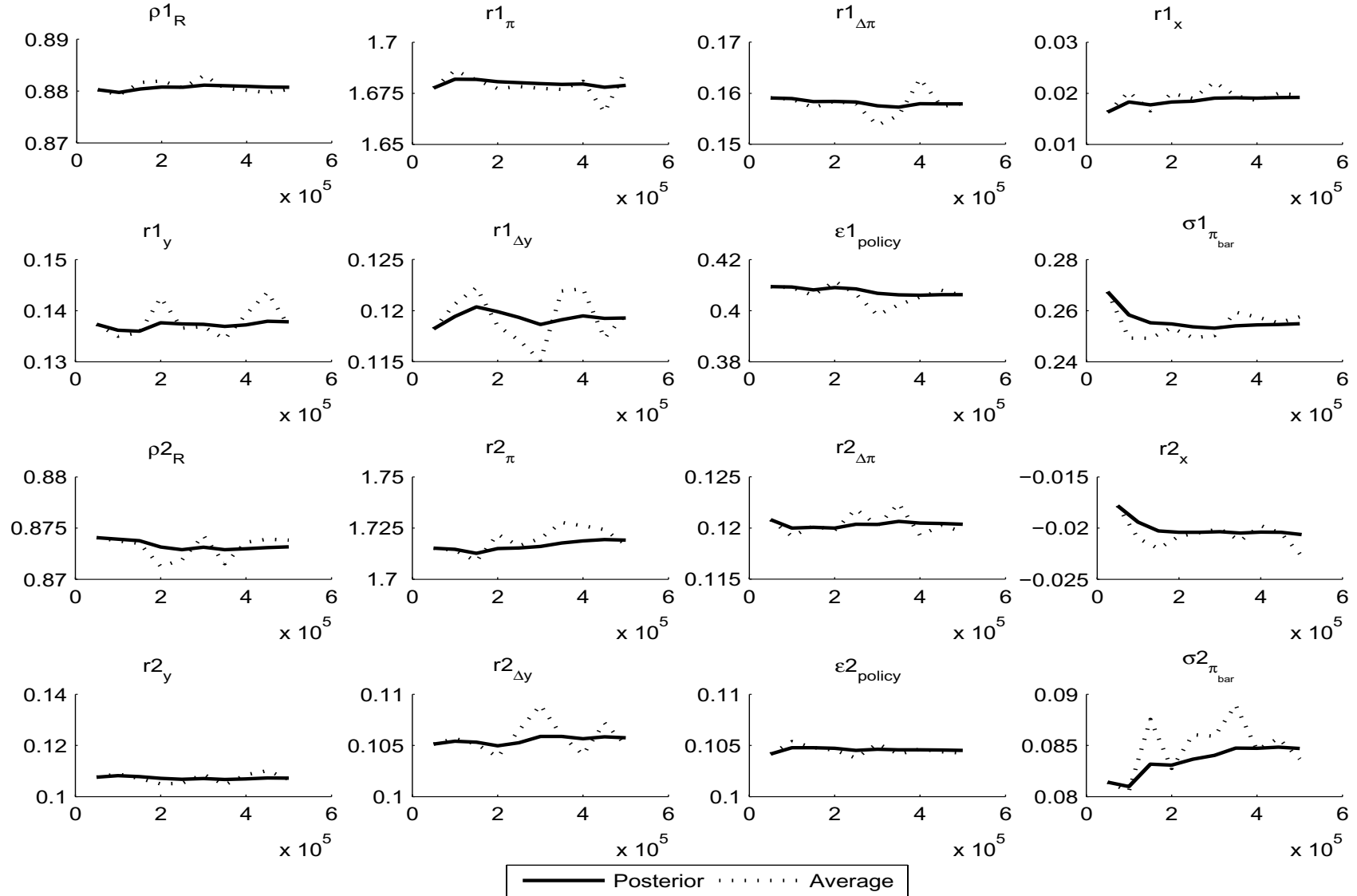


Figure A.4: Sequential marginal likelihoods.

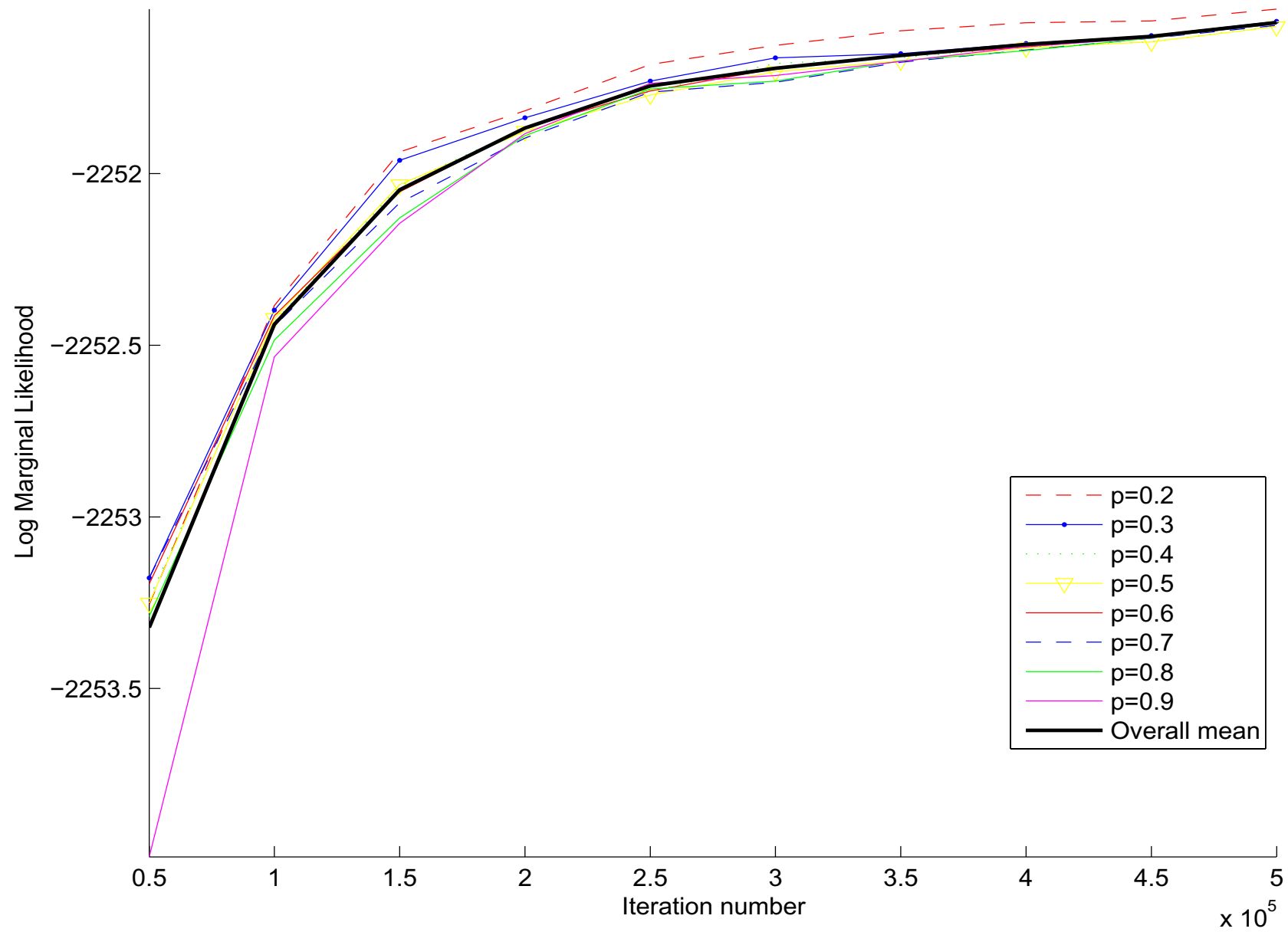
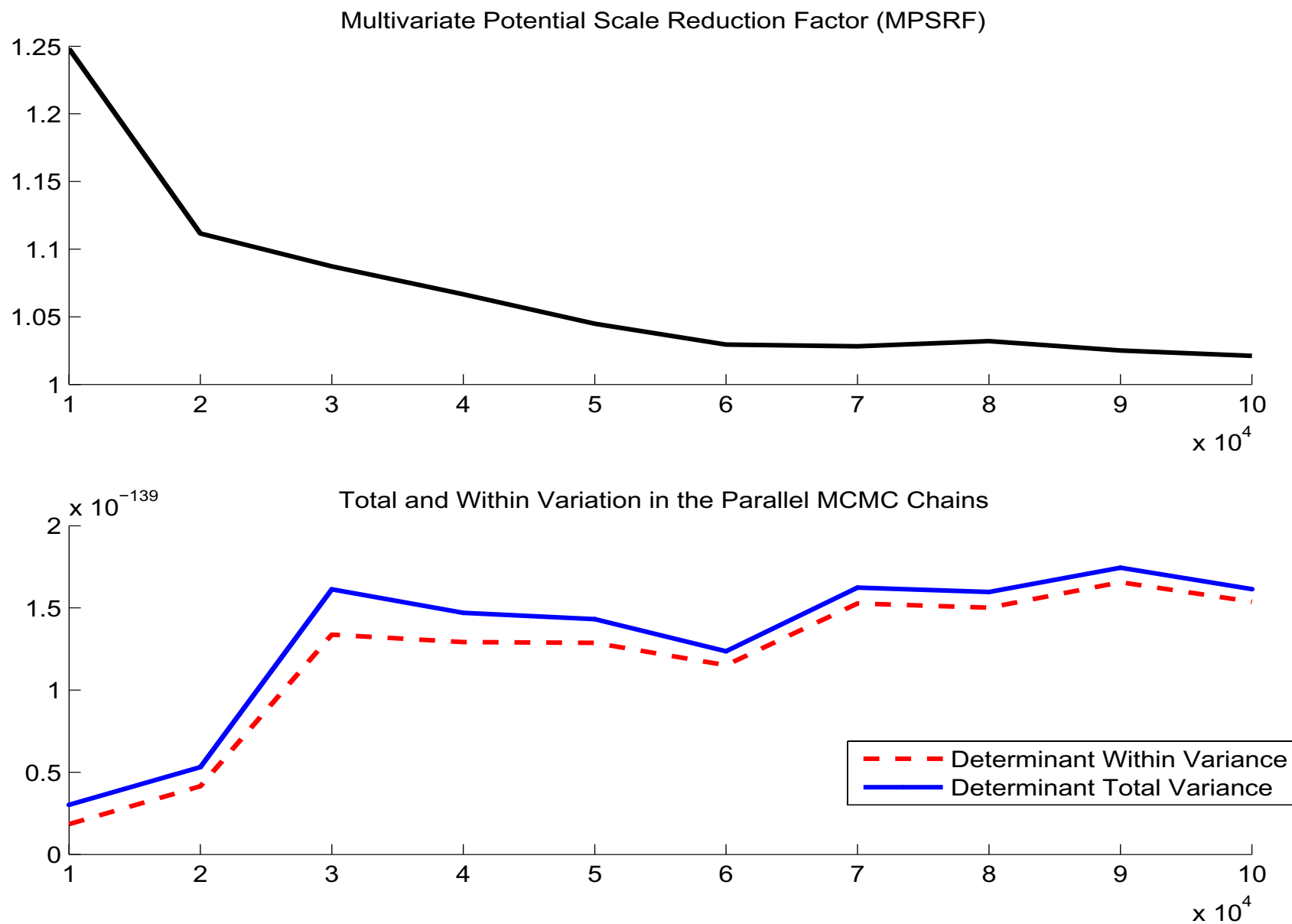


Figure A.5: Multivariate ANOVA.



Note: The analysis is based on four Metropolis chains with different initial values and 500,000 draws each, subsampling every 5th draw.

Figure A.6a: Log likelihood contours in the  $\{\tilde{\phi}_s, \rho_\phi\}$ -space, using all observable variables.

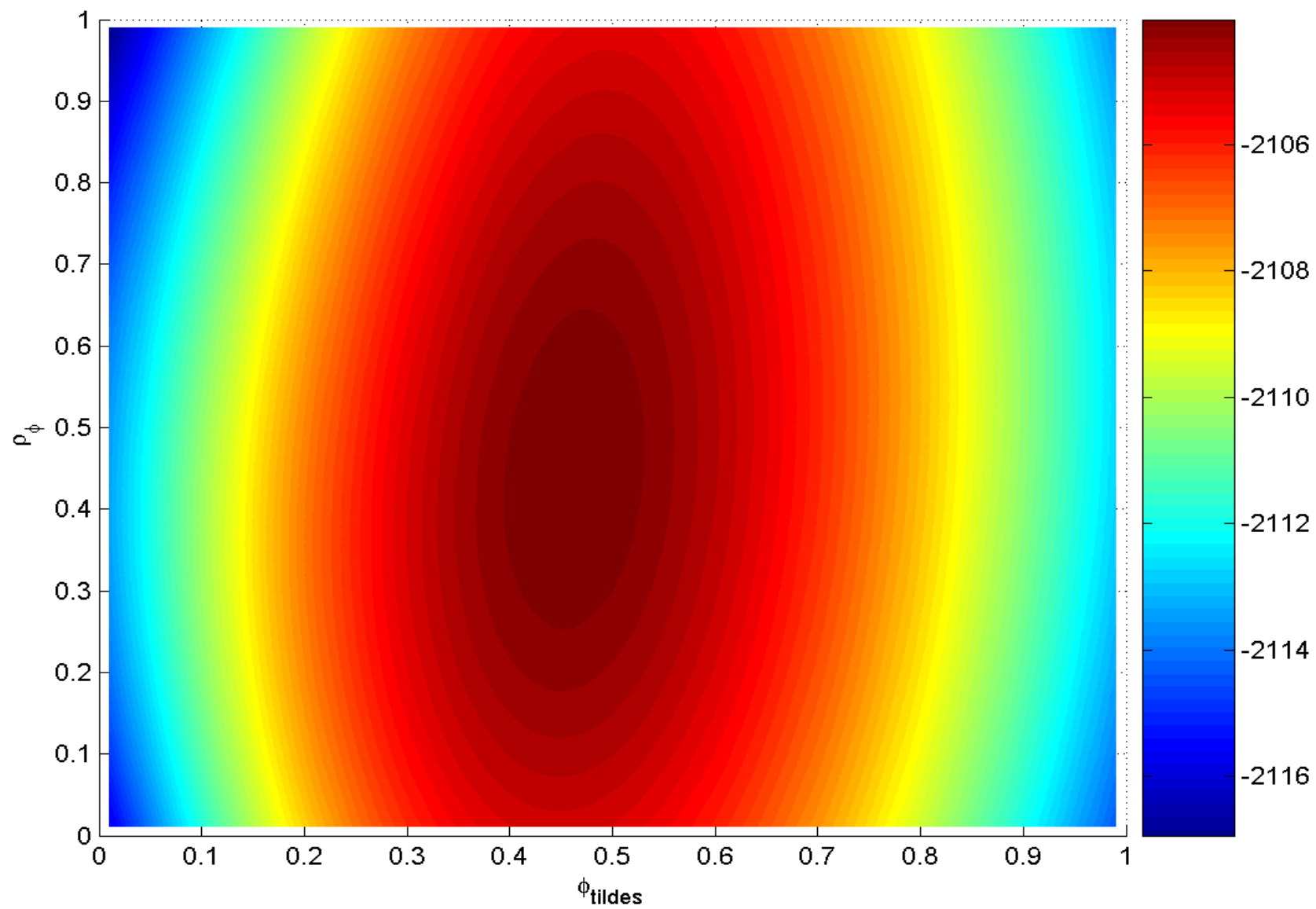


Figure A.6b: Log likelihood contours in the  $\{\tilde{\phi}_s, \rho_\phi\}$ -space, only using the real exchange rate.

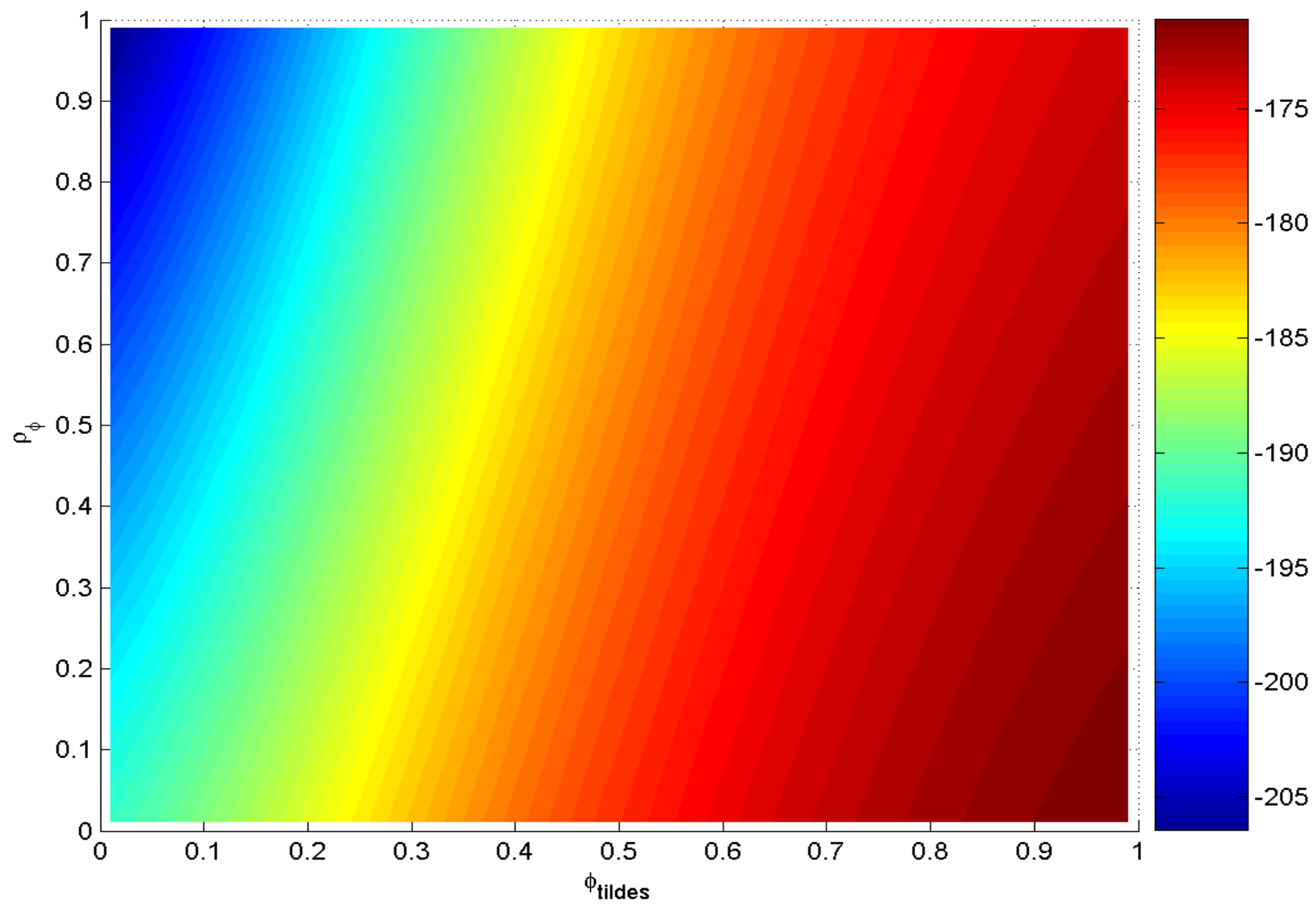


Figure A.7: Data (solid) and two-sided Kalman filtered estimates (dashed).

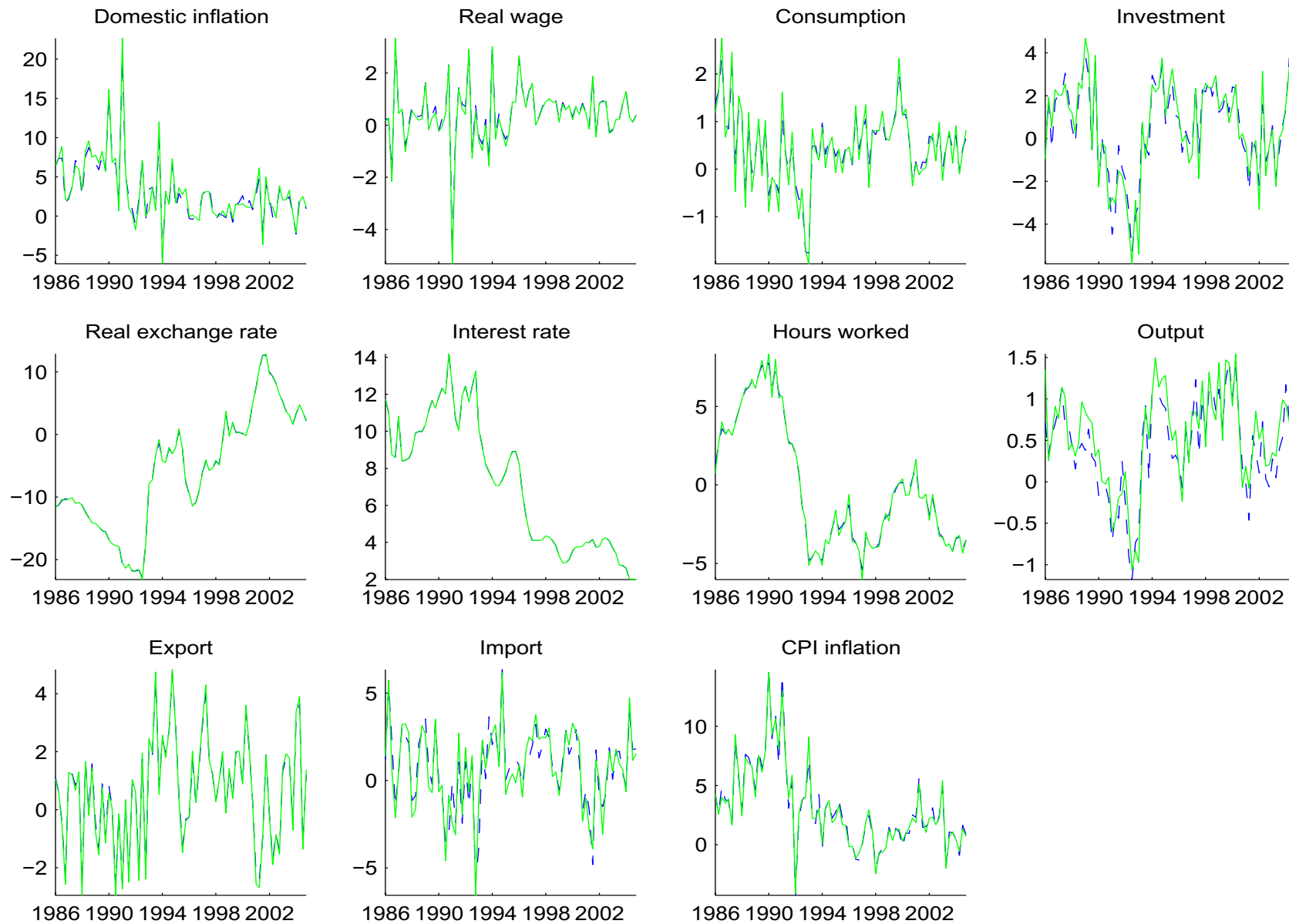


Figure A.8: Vector autocovariance functions in the DSGE model with the modified UIP condition (solid), DSGE-VAR  $\lambda = \infty$  (dotted) and DSGE-VECM  $\lambda = \infty$  (dashed).

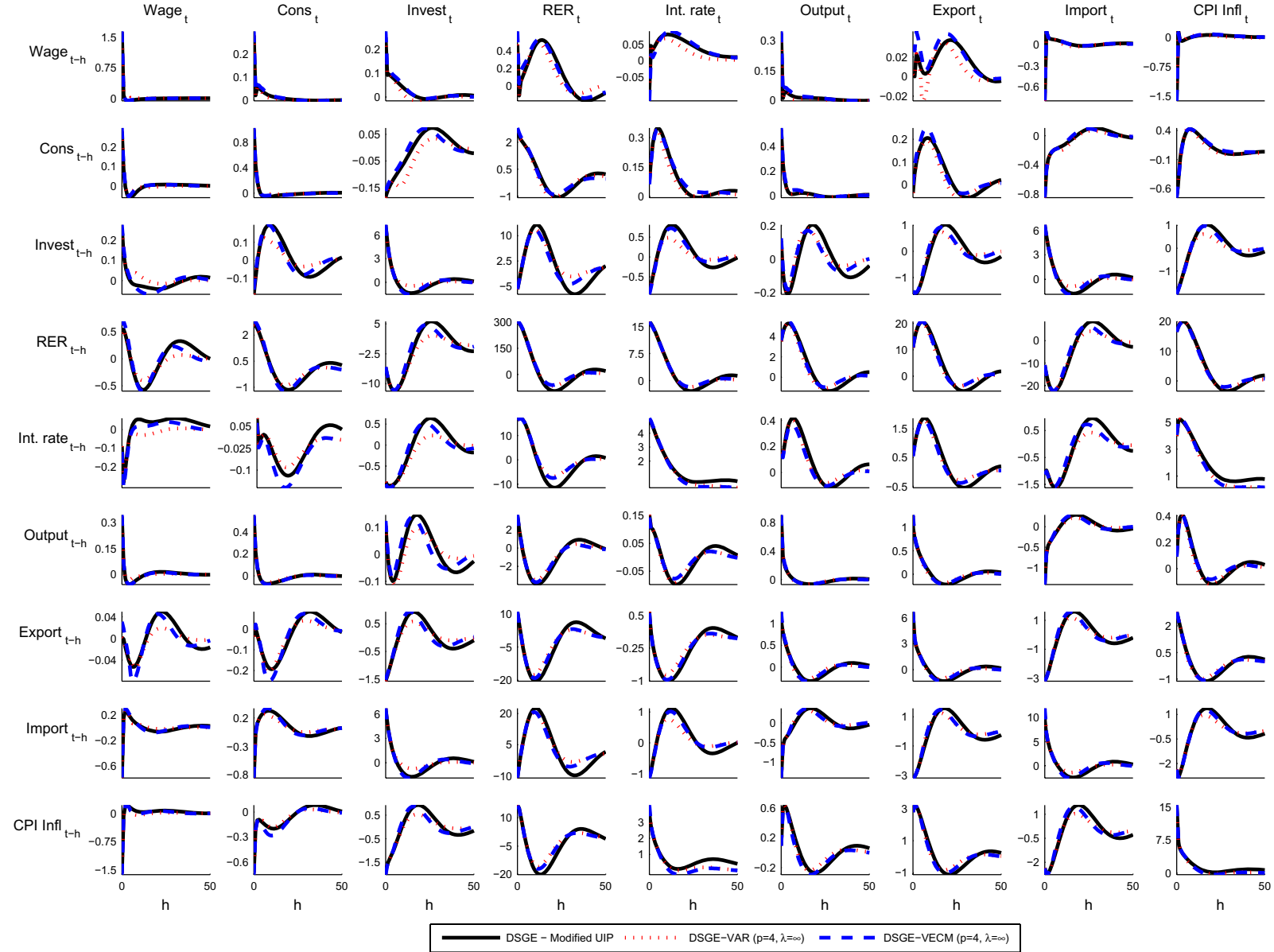


Figure A.9: Cross-correlation functions (CCF) from the DSGE-VECM  $\lambda=\hat{\lambda}$  with the UIP (solid) and the modified UIP (dashed) condition. The subgraphs below the diagonal display the cross-correlation between the column variable and the lag of the row variable. The opposite order applies to the upper diagonal graphs. The CCFs are computed at the posterior mode estimates of the parameters within each model. The numbers in the bottom of the graphs are the standard deviations of the respective variable in UIP case. The corresponding standard deviations for the model with the modified UIP condition are displayed to the right of the subgraphs.

